Paper

A Multiport Representation of the Step Junction of Two Circular Dielectric Waveguides and its Application to the Stepwise Approximation of a Tapered Dielectric Waveguide

Non-member Pirapaharan Kandasamy (Kinki University)
Non-member Nobuo Okamoto (Kinki University)

A multiport representation of the step junction of two circular dielectric waveguides of different size and its application to the stepwise approximation of a tapered dielectric waveguide are presented. Continuous spectral modes of the circular dielectric waveguide are discretized at a terminal plane by means of expressing their mode amplitudes in the form of infinite series of orthonormal Gaussian Laguerre functions. Applying the standard mode matching technique at the terminal plane, a rigorous multiport representation of the step junction of two circular dielectric waveguides is derived. Using the multiport representation, a stepwise approximate solution is given for the tapered dielectric waveguide. Numerical examples are given where the results are tested for the conservation of power. Also the numerical results are compared with those from Marcuse's approximate methods.

Keywords: Multiport representation, Step junction, Stepwise approximation, Tapered dielectric waveguide

1. Introduction

A tapered dielectric waveguide is an electromagnetic wave-guiding system used as a matching component connecting two waveguides of different size or dielectric antenna in lightwave and microwave engineering. Because of the practical importance of this configuration, it has been subject to several investigations[1]~[4].

A tapered dielectric waveguide such as a conical dielectric waveguide has a non-separable boundary surface by which we mean that the method of separation of variables can not be applied for the posed boundary value problem. Hence there is no analytical solution for this wave-guiding system except some approximate solutions.

So far typical approaches to the problem are Synder's coupled mode method[2][3] and Marcuse's radiation loss method[4]. These methods are effective but have some limitations. The former method is formulated under the condition that the flare-angle of the cone is very small and the latter one with some assumptions for the simplification purpose that the scattered power can be neglected while cascading an infinitesimal step junction of two circular dielectric rods. Therefore, a comprehensive and rigorous analysis on the tapered dielectric waveguide is really needed.

One of the approximate methods for a tapered dielectric waveguide is a stepwise approximate method. However the publications on this subject have not been found in the technical literature so far. In order to achieve an analytical solution using a stepwise approximate method, first a rigorous analysis on the step junction of two circular dielectric waveguides of different size is necessary.

In this paper, first, a comprehensive and rigorous multiport representation of the symmetric step junction of two circular dielectric waveguides of different size is derived and the next, a stepwise approximation to the circular conical dielectric waveguides is presented using the multiport representation of the symmetric step junction of two circular dielectric waveguides of different size.

The electromagnetic modes of discrete spectrum (called as discrete modes) and those of continuous spectrum (called as continuous modes) are reformulated in accordance with the transmission line equation. Thereby the normal mode amplitudes of discrete and continuous modes are formulated through the transmission equations.

The amplitudes of the continuous modes are expanded into an infinite series of complete orthonormal Gaussian Laguerre functions at the terminal plane, and thus discretized mode amplitudes are obtained. Such a technique has once been employed by Mohmoud and Beal[5]

in the analysis of a dielectric discontinuity of a planar waveguide. However, the concept of the port representation has not been used and the multiport representation also has not been given. Also a multimode network formulation of a step discontinuity has been given by M. Guglielmi *et al.*[6], but the formulation is applicable only to a rectangular waveguide.

Applying the boundary conditions at the terminal plane of the step junction, a comprehensive and rigorous multiport representation of the symmetric step junction of the two circular dielectric waveguide is derived. It is also noted that expanding the mode amplitude in the space function, T. E. Rozi has given a method of solution by a port representation for the step junction of planar dielectric waveguides[7].

Using the multiport representation of the step junction of two circular dielectric waveguides, a tapered dielectric waveguide has been analyzed by the stepwise approximate method, where a tapered dielectric waveguide is approximated as the cascading of step junctions and short sections of a cylindrical waveguide section. The overall transmission matrix has been given by the multiple products of each multiport stages.

Numerical examples are given for the single step junctions using multiport representation and the results are tested for the conservation of power. Also the results are compared with those of Marcuse's approximate methods.

Numerical examples are also given by cascading up to 4 stages when an incident field of HE_{11} is applied. Once again, the numerical results are compared with those obtained from Marcuse's radiation loss method.

2. Mode fields of a circular dielectric waveguide

〈2·1〉 **Discrete modes** The transverse electric field vector $\hat{E}_{tp}$ and magnetic field vector $\hat{H}_{tp}$ of the discrete spectrum for a circular dielectric waveguide of radius d are defined in the circular cylindrical coordinate system (r, ϕ, z), as follows:

$$\hat{E}_{tp}=V_p(z)\hat{e}_{tp} \quad \cdots\cdots(1)$$

$$\hat{H}_{tp}=I_p(z)\hat{h}_{tp} \quad \cdots\cdots(2)$$

and the longitudinal electric field components E_{zp} and magnetic field components H_{zp} are defined, as follows:

$$E_{zp}=\frac{1}{j\omega\varepsilon_0\varepsilon_r}I_p(z)\nabla_t\cdot(\hat{h}_{tp}\times\hat{i}_z) \quad \cdots\cdots(3)$$

$$H_{zp}=\frac{1}{j\omega\mu_0}V_p(z)\nabla_t\cdot(\hat{i}_z\times\hat{e}_{tp}) \quad \cdots\cdots(4)$$

where p is an integer specifying the mode and $\hat{i}_z$ denotes the unit vector in the z direction. Vectors $\hat{e}_{tp}$ and $\hat{h}_{tp}$ are mode functions which are determined in a manner so that Eqs. (1)～(4) satisfy the field equations subject to the boundary condition at the surface of the dielectric rod. Also, $\hat{e}_{tp}$ and $\hat{h}_{tp}$ satisfy the orthonormal relation at the entire transverse plane S (outside as well as inside the rod):

$$\int_S \hat{e}_{tp}\times\hat{h}_{tq}^*\cdot\hat{i}_z dS=\delta_{pq} \quad \cdots\cdots(5)$$

where $\hat{h}_{tp}^*$ denotes a complex conjugate of $\hat{h}_{tp}$, and δ_{pq} is Kronecker's delta, and also p, q indicate the arbitrary mode numbers. $V_p(z)$ and $I_p(z)$ are the p-th mode voltage and p-th mode current, respectively, and they satisfy the transmission line equations:

$$\frac{dV_p(z)}{dz}=-j\beta_p Z_0 I_p(z), \quad \frac{dI_p(z)}{dz}=-j\frac{\beta_p}{Z_0}V_p(z) \quad \cdots\cdots(6)$$

where β_p is the propagation constant of the p-th mode and $Z_0(=\sqrt{\mu_0/\varepsilon_0})$ is an intrinsic impedance of the free space. We denote the quantities in the region $0\leq r<d$ (inside the rod) as

$$\hat{e}_{tp}^{(i)},\ \hat{h}_{tp}^{(i)},\ \varepsilon_r^{(i)}$$

and those in the region $d\leq r$ (outside the rod) as

$$\hat{e}_{tp}^{(o)},\ \hat{h}_{tp}^{(o)},\ \varepsilon_r^{(o)}$$

Thus, the cylindrical components of $\hat{e}_{tp}^{(i),(o)}$ and $\hat{h}_{tp}^{(i),(o)}$ are expressed as follows:

$$e_{pr}^{(i),(o)}=-\frac{k_0}{2j\beta_p}\left[U_p^{(i),(o)}\frac{\beta_p^2}{k_0^2\varepsilon_r^{(i),(o)}}Z_m^{(i),(o)\prime}(k_{cp}^{(i),(o)}r)+W_p^{(i),(o)}\frac{m}{k_{cp}^{(i),(o)}r}Z_m^{(i),(o)}(k_{cp}^{(i),(o)}r)\right]e^{-jm\phi} \quad \cdots\cdots(7)$$

$$e_{p\phi}^{(i),(o)}=-\frac{k_0}{2\beta_p}\left[U_p^{(i),(o)}\frac{m\beta_p^2}{k_{ck}^{(i),(o)}k_0^2\varepsilon_r^{(i),(o)}r}Z_m^{(i),(o)}(k_{cp}^{(i),(o)}r)+W_p^{(i),(o)}Z_m^{(i),(o)\prime}(k_{cp}^{(i),(o)}r)\right]e^{-jm\phi} \quad \cdots\cdots(8)$$

$$h_{pr}^{(i),(o)}=\frac{1}{2}\left[U_p^{(i),(o)}\frac{m}{k_{cp}^{(i),(o)}r}Z_m^{(i),(o)}(k_{cp}^{(i),(o)}r)+W_p^{(i),(o)}Z_m^{(i),(o)\prime}(k_{cp}^{(i),(o)}r)\right]e^{-jm\phi} \quad \cdots\cdots(9)$$

$$h_{p\phi}^{(i),(o)}=\frac{1}{2j}\left[U_p^{(i),(o)}Z_m^{(i),(o)\prime}(k_{cp}^{(i),(o)}r)+W_p^{(i),(o)}\frac{m}{k_{cp}^{(i),(o)}r}Z_m^{(i),(o)}(k_{cp}^{(i),(o)}r)\right]e^{-jm\phi} \quad \cdots\cdots(10)$$

where m is an integer and $k_{cp}^{(i),(o)}=\sqrt{\varepsilon_r^{(i),(o)}k_0^2-\beta_p^2}$ and $k_0=\omega\sqrt{\varepsilon_0\mu_0}$. Moreover $Z_m^{(i)}=J_m$ and $Z_m^{(o)}=H_m^{(2)}$ are the Bessel function and Hankel function of the second kind, respectively. The coefficients $U_p^{(i)}$, $W_p^{(i)}$, $U_p^{(o)}$ and $W_p^{(o)}$ are evaluated from the boundary conditions at the surface of a dielectric rod. The time factor $e^{j\omega t}$ is assumed and suppressed throughout the equations.

Transforming $V_p(z)$ and $I_p(z)$ into normal mode amplitudes $a_p(z)$ and $b_p(z)$ through

$$V_p(z)=a_p(z)+b_p(z),\ Z_0I_p(z)=a_p(z)-b_p(z)\cdots(11)$$

we obtain uncoupled equations of mode amplitudes:

$$\frac{da_p(z)}{dz}=-j\beta_p a_p(z),\ \frac{db_p(z)}{dz}=j\beta_p b_p(z)\ \cdots\cdots(12)$$

Eigenvalue equation for the discrete modes of cylindrical rod as follows[8]:

$$(\varepsilon_r^{(i)}\breve{J}-\varepsilon_r^{(o)}\breve{H})(\breve{J}-\breve{H})=\left[\frac{m\beta_p k_0(\varepsilon_r^{(i)}-\varepsilon_r^{(o)})}{d^2k_{cp}^{(i)2}k_{cp}^{(o)2}}\right]^2 \cdots\cdots(13)$$

where $\breve{J}=\dfrac{J_m'(k_{cp}^{(i)}d)}{k_{cp}^{(i)}dJ_m(k_{cp}^{(i)}d)}$ and $\breve{H}=\dfrac{H_m^{(2)\prime}(k_{cp}^{(o)}d)}{k_{cp}^{(o)}dH_m^{(2)}(k_{cp}^{(o)}d)}$.

The dispersion curves obtained from Eq. (13) is shown in Fig. 1.

〈2・2〉 Continuous modes The transverse electric field vector $\bar{\bar{E}}_t$ and magnetic field vector $\bar{\bar{H}}_t$ of the continuous spectrum for a circular dielectric waveguide of radius d are defined in the circular cylindrical coordinate system (r, ϕ, z), as follows:

$$\bar{\bar{E}}_t=\bar{V}^H(z,\Gamma)\bar{\bar{e}}_t^H(r,\phi,\Gamma)+\bar{V}^{HE}(z,\Gamma)\bar{\bar{e}}_t^{HE}(r,\phi,\Gamma) \cdots\cdots(14)$$

$$\bar{\bar{H}}_t=\bar{I}^H(z,\Gamma)\bar{\bar{h}}_t^H(r,\phi,\Gamma)+\bar{I}^{HE}(z,\Gamma)\bar{\bar{h}}_t^{HE}(r,\phi,\Gamma) \cdots\cdots(15)$$

and the longitudinal electric field components $\bar{E}_z$ and magnetic field components $\bar{H}_z$ are defined, as follows:

$$\bar{E}_z=\frac{1}{j\omega\varepsilon_0\varepsilon_r}\bar{I}^H(z,\Gamma)\nabla_t\cdot(\bar{\bar{h}}_t^H(r,\phi,\Gamma)\times\hat{i}_z)+\frac{1}{j\omega\varepsilon_0\varepsilon_r}\bar{I}^{HE}(z,\Gamma)\nabla_t\cdot(\bar{\bar{h}}_t^{HE}(r,\phi,\Gamma)\times\hat{i}_z) \cdots\cdots(16)$$

$$\bar{H}_z=\frac{1}{j\omega\mu_0}\bar{V}^H(z,\Gamma)\nabla_t\cdot(\hat{i}_z\times\bar{\bar{e}}_t^H(r,\phi,\Gamma))+\frac{1}{j\omega\mu_0}\bar{V}^{HE}(z,\Gamma)\nabla_t\cdot(\hat{i}_z\times\bar{\bar{e}}_t^{HE}(r,\phi,\Gamma)) \cdots\cdots(17)$$

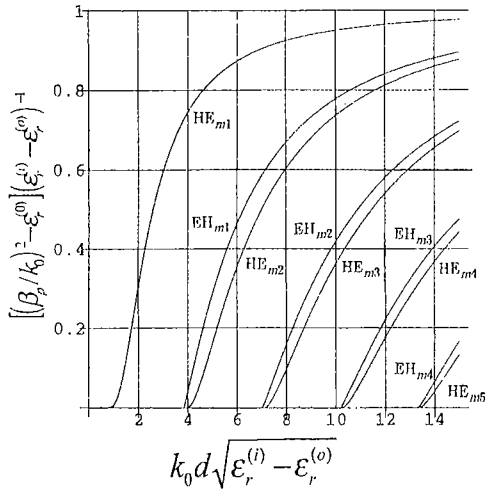

Fig. 1 Dispersion curves of a circular delectric wagvuide ($\varepsilon_r^{(i)}=2$, $\varepsilon_r^{(o)}=1$ and $m=1$).

where Γ is the normalized transverse propagation constant defined by

$$\Gamma=k_c^{(o)}d=d\sqrt{\varepsilon_r^{(o)}k_0^2-\beta^2}.$$

Two kinds of mutually orthogonal continuous spectral mode functions:

$$(\bar{\bar{e}}_t^H,\ \bar{\bar{h}}_t^H);\ (\bar{\bar{e}}_t^{HE},\ \bar{\bar{h}}_t^{HE})$$

are selected and those are determined from the field equations and the electromagnetic field boundary conditions at the surface of the dielectric rod. They are also subject to the orthogonality relations:

$$\int_S\bar{\bar{e}}_t^{(H_{HE})}(r,\phi,\Gamma)\times\bar{\bar{h}}_t^{(H_{HE})^*}(r,\phi,\Gamma')\cdot\hat{i}_z dS=f_\beta\delta\left(\frac{k_c^{(o)}}{k_0}-\frac{k_c^{(o)\prime}}{k_0}\right)\quad\begin{cases}f_\beta=1(\beta:\text{ real})\\ f_\beta=\pm j(\beta:\text{ imaginary})\end{cases} \cdots\cdots(18)$$

as well as the mutually orthogonal conditions:

$$\int_S\bar{\bar{e}}_t^{(H_{HE})}(r,\phi,\Gamma)\times\bar{\bar{h}}_t^{(HE_H)^*}(r,\phi,\Gamma')\cdot\hat{i}_z ds=0 \cdots\cdots(19)$$

where the integration is performed on the entire transverse plane S (inside as well as outside the rod), and $\Gamma'=k_c^{(o)\prime}d=d\sqrt{\varepsilon_r^{(o)}k_0^2-\beta'^2}$. $\delta(\ )$ denotes the delta function. The mode voltage $\bar{V}(z,\Gamma)$ and mode current $\bar{I}(z,\Gamma)$ satisfy the transmission line equations:

$$\left.\begin{aligned}\frac{d\bar{V}(z,\Gamma)}{dz}&=-j\beta(\Gamma)Z_0\bar{I}(z,\Gamma)\\ \frac{d\bar{I}(z,\Gamma)}{dz}&=-j\frac{\beta(\Gamma)}{Z_0}\bar{V}(z,\Gamma)\end{aligned}\right\} \cdots\cdots(20)$$

where $\bar{V}(z,\Gamma)$ and $\bar{I}(z,\Gamma)$ imply $\bar{V}^H(z,\Gamma)$ or $\bar{V}^{HE}(z,\Gamma)$ and $\bar{I}^H(z,\Gamma)$ or $\bar{I}^{HE}(z,\Gamma)$, respectively. Transformation for $\bar{V}(z,\Gamma)$ and $\bar{I}(z,\Gamma)$ into $\bar{a}(z,\Gamma)$ and $\bar{b}(z,\Gamma)$ through

$$\left.\begin{aligned}\bar{V}(z,\Gamma)&=\bar{a}(z,\Gamma)+\bar{b}(z,\Gamma)\\ Z_0I(z,\Gamma)&=\bar{a}(z,\Gamma)-b(z,\Gamma)\end{aligned}\right\} \cdots\cdots(21)$$

yields the uncoupled equations of mode amplitudes as follows:

$$\frac{d\bar{a}(z,\Gamma)}{dz}=-j\beta(\Gamma)\bar{a}(z,\Gamma),\ \frac{d\bar{b}(z,\Gamma)}{dz}=j\beta(\Gamma)\bar{b}(z,\Gamma) \cdots\cdots(22)$$

where $\bar{a}(z,\Gamma)$ and $\bar{b}(z,\Gamma)$ imply $\bar{a}^H(z,\Gamma)$ or $\bar{a}^{HF}(z,\Gamma)$ and $\bar{b}^H(z,\Gamma)$ or $\bar{b}^{HE}(z,\Gamma)$, respectively.

The cylindrical components of vector mode functions are as follows:

Inside the rod $(0\le r<d)$:

$$\bar{e}_r^{(i)H,HE}=\frac{k_0}{2j\beta}\left[\bar{U}^{(i)H,HE}\frac{\beta^2}{k_0^2\varepsilon_r^{(i)}}J_m'(k_c^{(i)}r)+\bar{W}^{(i)H,HE}\frac{m}{k_c^{(i)}r}J_m(k_c^{(i)}r)\right]e^{-jm\phi} \cdots\cdots(23)$$

$$\bar{e}_\phi^{(i)H,HE}=-\frac{k_0}{2\beta}\left[\bar{U}^{(i)H,HE}\frac{m\beta^2}{k_c^{(i)}k_0^2\varepsilon_r^{(i)}r}J_m(k_c^{(i)}r)+\bar{W}^{(i)H,HE}J_m'(k_c^{(i)}r)\right]e^{-jm\phi} \cdots\cdots(24)$$

$$\bar{h}_r^{(i)H,HE}=\frac{1}{2}\left[\begin{array}{l}\bar{U}^{(i)H,HE}\dfrac{m}{k_c^{(i)}r}J_m(k_c^{(i)}r)\\ +\bar{W}^{(i)H,HE}J_m'(k_c^{(i)}r)\end{array}\right]e^{-jm\phi} \quad \cdots\cdots(25)$$

$$\bar{h}_\phi^{(i)H,HE}=\frac{1}{2j}\left[\begin{array}{l}\bar{U}^{(i)H,HE}J_m'(k_c^{(i)}r)\\ +\bar{W}^{(i)H,HE}\dfrac{m}{k_c^{(i)}r}J_m(k_c^{(i)}r)\end{array}\right]e^{-jm\phi} \quad \cdots\cdots(26)$$

Outside rod ($d\leq r$):

$$\bar{e}_r^{(o)H,HE}=\frac{k_0}{2j\beta}\left[\begin{array}{l}\dfrac{\beta^2}{k_0^2\varepsilon_r^{(o)}}\left(\begin{array}{l}\bar{U}^{(o)H,HE}H_m^{(2)\prime}(k_c^{(o)}r)\\ +\bar{\bar{U}}^{(o)H,HE}H_m^{(1)\prime}(k_c^{(o)}r)\end{array}\right)\\ +\dfrac{m}{k_c^{(o)}r}\left(\begin{array}{l}\bar{W}^{(o)H,HE}H_m^{(2)}(k_c^{(o)}r)\\ +\bar{\bar{W}}^{(o)H,HE}H_m^{(1)}(k_c^{(o)}r)\end{array}\right)\end{array}\right]e^{-jm\phi} \quad \cdots\cdots(27)$$

$$\bar{e}_\phi^{(o)H,HE}=\frac{-k_0}{2\beta}\left[\begin{array}{l}\dfrac{m\beta^2}{k_c^{(o)}k_0^2\varepsilon_r^{(o)}r}\left(\begin{array}{l}\bar{U}^{(o)H,HE}H_m^{(2)}(k_c^{(o)}r)\\ +\bar{\bar{U}}^{(o)H,HE}H_m^{(1)}(k_c^{(o)}r)\end{array}\right)\\ +\left(\begin{array}{l}\bar{W}^{(o)H,HE}H_m^{(2)}(k_c^{(o)}r)\\ +\bar{\bar{W}}^{(o)H,HE}H_m^{(1)}(k_c^{(o)}r)\end{array}\right)\end{array}\right]e^{-jm\phi} \quad \cdots\cdots(28)$$

$$\bar{h}_r^{(o)H,HE}=\frac{1}{2}\left[\begin{array}{l}\dfrac{m}{k_c^{(o)}r}\left(\begin{array}{l}\bar{U}^{(o)H,HE}H_m^{(2)}(k_c^{(o)}r)\\ +\bar{\bar{U}}^{(o)H,HE}H_m^{(1)}(k_c^{(o)}r)\end{array}\right)\\ +\left(\begin{array}{l}\bar{W}^{(o)H,HE}H_m^{(2)}(k_c^{(o)}r)\\ +\bar{\bar{W}}^{(o)H,HE}H_m^{(1)}(k_c^{(o)}r)\end{array}\right)\end{array}\right]e^{-jm\phi} \quad \cdots\cdots(29)$$

$$\bar{h}_\phi^{(i)H,HE}=\frac{1}{2j}\left[\begin{array}{l}\left(\begin{array}{l}\bar{U}^{(o)H,HE}H_m^{(2)\prime}(k_c^{(0)}r)\\ +\bar{\bar{U}}^{(o)H,HE}H_m^{(1)\prime}(k_c^{(o)}r)\end{array}\right)\\ +\dfrac{m}{k_c^{(o)}r}\left(\begin{array}{l}\bar{W}^{(o)H,HE}H_m^{(2)}(k_c^{(o)}r)\\ +\bar{\bar{W}}^{(o)H,HE}H_m^{(1)}(k_c^{(o)}r)\end{array}\right)\end{array}\right]e^{-jm\phi} \quad \cdots\cdots(30)$$

where $k_c^{(i)}=\sqrt{\varepsilon_r^{(i)}k_0^2-\beta^2}$ and J_m, $H_m^{(1)}$ and $H_m^{(2)}$ are the Bessel function, Hankel function of the first kind and second kind, respectively. Further, the coefficients ($\bar{U}^{(i)H}$, $\bar{W}^{(i)H}$, $\bar{\bar{U}}^{(o)H}$, $\bar{\bar{U}}^{(o)H}$, $\bar{W}^{(o)H}$, $\bar{\bar{W}}^{(o)H}$) and ($\bar{U}^{(i)HE}$, $\bar{W}^{(i)HE}$, $\bar{U}^{(o)HE}$, $\bar{\bar{U}}^{(o)HE}$, $\bar{W}^{(o)HE}$, $\bar{\bar{W}}^{(o)HE}$) have to be obtained from the boundary condition at $r=d$, the normalization condition given by Eq. (18) for each modes (named as H and HE) and the orthonormal condition between H and HE modes given by Eq. (19). Here it is also defined that $\bar{U}^{(i)H}=0$, since the coefficients can be determined infinitely many ways[4][9].

3. Multiport representation of the step junction

Fig. 2 shows the symmetric step junction of the two circular dielectric waveguides. Total field expressions for the transverse fields in the waveguide I and II are given by the summation of discrete spectral modes expressed by Eqs. (1) and (2), and the continuous spectral modes expressed by Eqs. (14) and (15) in each region, as follows:

$$\begin{aligned}\hat{E}_t^{\mathrm{I,II}}=&\sum_{p=1}^{N_d^{\mathrm{I,II}}}(a_p^{\mathrm{I,II}}(z)+b_p^{\mathrm{I,II}}(z))\hat{e}_{tp}^{\mathrm{I,II}}(r,\phi)\\ &+\int_0^\infty(\bar{a}^{H\mathrm{I},H\mathrm{II}}(z,\Gamma^{\mathrm{I,II}})\\ &+\bar{b}^{H\mathrm{I},H\mathrm{II}}(z,\Gamma^{\mathrm{I,II}}))\bar{\bar{e}}_t^{H}(r,\phi,\Gamma^{\mathrm{I,II}})\mathrm{d}\Gamma^{\mathrm{I,II}}\\ &+\int_0^\infty(\bar{a}^{HE\mathrm{I},HE\mathrm{II}}(z,\Gamma^{\mathrm{I,II}})\\ &+\bar{b}^{HE\mathrm{I},HE\mathrm{II}}(z,\Gamma^{\mathrm{I,II}}))\bar{\bar{e}}^{HE}(r,\phi,\Gamma^{\mathrm{I,II}}))\mathrm{d}\Gamma^{\mathrm{I,II}}\end{aligned} \quad \cdots\cdots(31)$$

$$\begin{aligned}Z_0\hat{H}_t^{\mathrm{I,II}}=&\sum_{p=1}^{N_d^{\mathrm{I,II}}}(a_p^{\mathrm{I,II}}(z)-b_p^{\mathrm{I,II}}(z))\hat{h}_{tp}^{\mathrm{I,II}}(r,\phi)\\ &+\int_0^\infty(\bar{a}^{H\mathrm{I},H\mathrm{II}}(z,\Gamma^{\mathrm{I,II}})\\ &-\bar{b}^{H\mathrm{I},H\mathrm{II}}(z,\Gamma^{\mathrm{I,II}}))\bar{\bar{h}}_t^{H}(r,\phi,\Gamma^{\mathrm{I,II}})\mathrm{d}\Gamma^{\mathrm{I,II}}\\ &+\int_0^\infty(\bar{a}^{HE\mathrm{I},HE\mathrm{II}}(z,\Gamma^{\mathrm{I,II}})\\ &-\bar{b}^{HE\mathrm{I},HE\mathrm{II}}(z,\Gamma^{\mathrm{I,II}}))\bar{\bar{h}}_t^{HE}(r,\phi,\Gamma^{\mathrm{I,II}})\mathrm{d}\Gamma^{\mathrm{I,II}}\end{aligned} \quad \cdots\cdots(32)$$

where superscript I and II stand for the quantities in the waveguides I and II, respectively. $N_d^{\mathrm{I,II}}$ indicates the number of discrete modes of propagation in the waveguides either I or II.

Using Eqs. (31) and (32) and applying the boundary condition at the terminal plane T_1, integral equations of mode amplitudes can be derived. However, solving those integral equations are the most difficult barrier. So, expanding continuous mode amplitudes which are continuous functions of normalized transverse propagation constant (Γ) by the complete orthonormal function of Γ, we obtain the discretized modes at a terminal plane. We adopt the set of Gaussian Laguerre functions as the complete set of orthonormal functions as Goubau *et al.*[10] do. Thereby those integral equations are transformed into algebraic equations. The mode amplitudes, $\bar{a}^{H\mathrm{I}}(z_1,\Gamma^{\mathrm{I}})$, etc. are expanded by Gaussian Laguerre functions:

$$\Psi_n(\lambda\Gamma)=e^{-\lambda\Gamma/2}L_n(\lambda\Gamma)\quad(n=1,2,3,\ldots)$$

as follows:

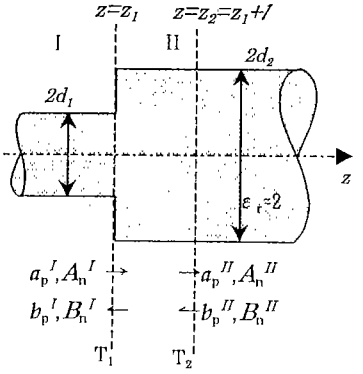

Fig. 2 Step junction of two circular dielectric waveguides.

$$\left.\begin{aligned}\bar{a}^{XI}(z_1, \Gamma^I)&=\sum_n A_n^{XI}(z_1)\Psi_n(\lambda\Gamma^I)\\ \bar{a}^{XII}(z_2, \Gamma^{II})&=\sum_n A_n^{XII}(z_2)\Psi_n(\lambda\Gamma^{II})\end{aligned}\right\} \cdots\cdots (33)$$

where the superscript X stands for H or HE and $L_n(\lambda\Gamma)$ is the Laguerre function of order n. λ is also a scale factor. In case of $\bar{b}^{XI}(z_1, \Gamma^I)$, etc. we replace $\bar{a}$ and A_n for $\bar{b}$ and B_n, respectively.

The unknown mode amplitudes A_n's and B_n's are determined by matching the transverse fields at terminal plane T_1. Applying Eq. (33) in Eqs. (31) and (32) and using the boundary conditions $\hat{E}^I=\hat{E}^{II}$ and $\hat{H}^I=\hat{H}^{II}$ at terminal plane T_1, we obtain that

$$\begin{aligned}&\sum_{p=1}^{N_0^I}(a_p^I(z_1)+b_p^I(z_1))\hat{e}_{tp}^I(r, \phi)\\ &+\sum_{n=0}^{\infty}(A_n^{HI}(z_1)+B_n^{HI}(z_1))\hat{\mathcal{E}}_n^{HI}(r, \phi)\\ &+\sum_{n=0}^{\infty}(A_n^{HEI}(z_1)+B_n^{HEI}(z_1))\hat{\mathcal{E}}_n^{HEI}(r, \phi)\\ &=\sum_{p=1}^{N_0^{II}}(a_p^{II}(z_2)e^{j\beta_p^{II}l}+b_p^{II}(z_2)e^{-j\beta_p^{II}l})\hat{e}_{tp}^{II}(r, \phi)\\ &+\sum_{n=0}^{\infty}A_n^{HII}(z_2)\hat{\mathcal{E}}_n^{HII+}(r, \phi)+\sum_{n=0}^{\infty}B_n^{HII}(z_2)\hat{\mathcal{E}}_n^{HII-}(r, \phi)\\ &+\sum_{n=0}^{\infty}A_n^{HEII}(z_2)\hat{\mathcal{E}}_n^{HEII+}+(r, \phi)\\ &+\sum_{n=0}^{\infty}B_n^{HEII}(z_2)\hat{\mathcal{E}}_n^{HEII-}-(r, \phi)\cdots\cdots (34)\end{aligned}$$

for transverse electric field, and

$$\begin{aligned}&\sum_{p=1}^{N_0^I}(a_p^I(z_1)-b_p^I(z_1))\hat{h}_{tp}^I(r, \phi)\\ &+\sum_{n=0}^{\infty}(A_n^{HI}(z_1)-B_n^{HI}(z_1))\hat{\mathcal{H}}_n^{HI}(r, \phi)\\ &+\sum_{n=0}^{\infty}(A_n^{HEI}(z_1)-B_n^{HEI}(z_1))\hat{\mathcal{H}}_n^{HEI}(r, \phi)\\ &=\sum_{p=1}^{N_0^{II}}(a_p^{II}(z_2)e^{j\beta_p^{II}l}-b_p^{II}(z_2)e^{-j\beta_p^{II}l})\hat{h}_{tp}^{II}(r, \phi)\\ &+\sum_{n=0}^{\infty}A_n^{HII}(z_2)\hat{\mathcal{H}}_n^{HII+}(r, \phi)\\ &-\sum_{n=0}^{\infty}B_n^{HII}(z_2)\hat{\mathcal{H}}_n^{HII-}(r, \phi)+\sum_{n=0}^{\infty}A_n^{HEII}(z_2)\hat{\mathcal{H}}_n^{HEII+}(r, \phi)\\ &-\sum_{n=0}^{\infty}B_n^{HEII}(z_2)\hat{\mathcal{H}}_n^{HEII-}(r, \phi)\cdots\cdots (35)\end{aligned}$$

for transverse magnetic field, where $(\hat{\mathcal{E}}_n^{HI}, \hat{\mathcal{E}}_n^{HEI}, \hat{\mathcal{E}}_n^{HII+}, \hat{\mathcal{E}}_n^{HII-}, \hat{\mathcal{E}}_n^{HEII+}, \hat{\mathcal{E}}_n^{HEII-})$ and $(\hat{\mathcal{H}}_n^{HI}, \hat{\mathcal{H}}_n^{HEI}, \hat{\mathcal{H}}_n^{HII+}, \hat{\mathcal{H}}_n^{HII-}, \hat{\mathcal{H}}_n^{HEII+}, \hat{\mathcal{H}}_n^{HEII-})$ are the transforms used for the simplicity of the equations in electric and magnetic field expressions, respectively. The expressions for the transforms are given by replacing $\hat{\mathcal{G}}$ and $\hat{g}$ for $\hat{\mathcal{E}}$ and $\hat{e}$ or $\hat{\mathcal{H}}$ and $\hat{h}$, respectively, as follows.

$$\begin{aligned}\hat{\mathcal{G}}_n^{XI}(r, \phi)&=\int_0^{\infty}\Psi_n(\lambda\Gamma^I)\bar{g}_t^X(\Gamma^I, r, \phi)d\Gamma^I\\ \hat{\mathcal{G}}_n^{XII+}(r, \phi)&=\int_0^{\infty}e^{j\beta(\Gamma^{II})l}\Psi_n(\lambda\Gamma^{II})\bar{g}_t^X(\Gamma^{II}, r, \phi)d\Gamma^{II}\\ \hat{\mathcal{G}}_n^{XII-}(r, \phi)&=\int_0^{\infty}e^{-j\beta(\Gamma^{II})l}\Psi_n(\lambda\Gamma^{II})\bar{g}_t^X(\Gamma^{II}, r, \phi)d\Gamma^{II}\end{aligned}$$

where X stands for H or HE. Using the orthogonality between the discrete and continuous spectral modes as well as the mutual orthgonality between the continuous spectral modes, Eqs. (34) and (35) are simplified as a multiport representation of the step junction as follows:

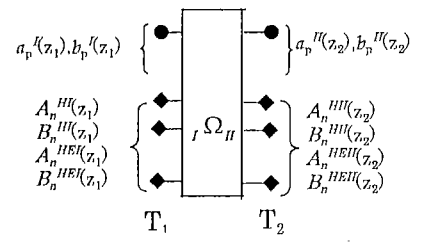

Fig. 3 Multiport representation of the step junction of circular dielectric waveguides.

$$\begin{bmatrix}[a_p^I(Z_1)]\\ [A_n^{HI}(z_1)]\\ [A_n^{HEI}(z_1)]\\ [b_p^I(z_1)]\\ [B_n^{HI}(z_1)]\\ [B_n^{HEI}(z_1)]\end{bmatrix}=[{}_I\Omega_{II}]\begin{bmatrix}[a_p^{II}(z_2)]\\ [A_n^{HII}(z_2)]\\ [A_n^{HEII}(z_2)]\\ [b_p^{II}(z_2)]\\ [B_n^{HII}(z_2)]\\ [B_n^{HEII}(z_2)]\end{bmatrix}\cdots\cdots (36)$$

The matrix form given above is a complete and rigorous representation for the step junction of a circular dielectric waveguides. $[{}_I\Omega_{II}]$ is the transmission matrix. The port representation is rigorous in principle only if an infinite number of expanding terms are explicitly included. However, for engineering applications, one can truncate the transmission matrix to a finite size as shown later.

4. Stepwise approximation of a tapered dielectric waveguide

A circular conical dielectric waveguide used as a tapered waveguide has a non-separable boundary surface that rejects the application of the method of separation of variables to the posed boundary value problems. Therefore we have to rely on the approximate method for an analysis of such guiding system. We here adopt the stepwise approximation method that the tapered dielectric rod is approximated by the cascading of the step junction of two circular dielectric waveguides followed by a short section of the waveguide. Here, we define two terminal planes T_1 and T_2, as shown in Fig. 2, in order to include the short sections of the waveguide II. In this case, the length of the short section can not be selected arbitrarily since it effects the numerical convergence of infinite integrals. Thus the stepwise approximation can be represented as a multiple cascading of the multiports of each stage as shown in Fig. 4. Therefore, the overall transmission matrix $[\Omega]$ for a multistage is given as follows:

$$[\Omega]=[{}_I\Omega_{II}]\cdot[{}_{II}\Omega_{III}]\cdots\cdots (37)$$

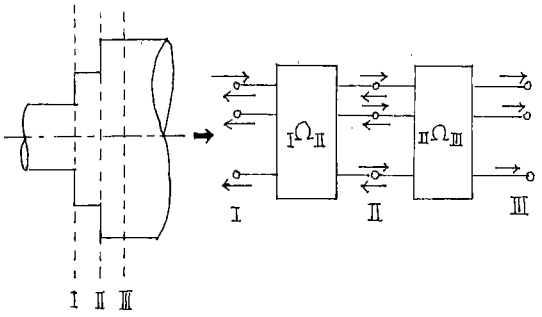

Fig. 4 Cascading of the mulitiport of each stage.

5. Numerical results

〈5·1〉 Single stage (step junction with a short waveguide section) To perform the numerical calculations, we truncate all the infinite series to a finite series. The size of the series is determined by the accuracy required for the numerical computation.

The matrix elements of the transmission matrix are numerically computed for two cases. One is for $d_2/d_1=1.05$, and the other for $d_2/d_1=2.00$. Both cases are being selected with in the range where the existence discrete mode is only dominant discrete mode (HE_{11}). Further, the number of terms in the series of discretized continuous spectral modes (H and HE) have been limited to 10 each. The data for convergence of mode amplitudes are given elsewhere[11].

Normalized powers of the discrete as well as continuous modes in both transmission and reflection sides are also determined separately and tested for the conservation of power as given in Table 1. Throughout the tables T and R indicate the transmitted and reflected, respectively. The error in the conservation of power is noticed 0.002% for $d_2/d_1=1.05$, and 0.8% for $d_2/d_1=2.00$, which can be improved by increasing the number of expansion terms while trading with the computation time.

The comparison of various power components with those from Marcuse's approximate "mode matching" and "radiation loss" methods is given in Table 2 and Table 3, respectively.

In Table 2, the transmitted power and reflected power of discrete modes calculated by Marcuse's mode-matching method are denoted, where the reflected components of continuous modes are neglected as done by Marcuse. In Table 3, the transmitted power and reflected power of continuous modes calculated by Marcuse's radiation-loss method are denoted, where the reflected components of discrete mode are neglected as done by Marcuse. Numerical results calculated from Marcuse's method and present method have good

Table 1. Test of conservation of power ($k_0d1=0.05$).

Power spectrum		$d_2/d_1=1.05$	$d_2/d_1=2.00$
T	Discrete	0.983883	0.430957
	Continuous	$0.160898*10^{-1}$	0.559534
R	Discrete	$0.528545*10^{-6}$	$0.304118*10^{-3}$
	Continuous	$0.446487*10^{-5}$	$0.136037*10^{-2}$
Total		0.999978	0.992155

Table 2. Comparison of present method with marcuse's mode matching method ($k_0d_1=1.00$ and $k_0l=0.05$).

Power in the discrete spectrum		$d_2/d_1=1.05$	$d_2/d_1=2.00$
T	Present	0.983883	0.430957
	Marcuse	0.981920	0.417789
R	Present	$0.528545*10^{-6}$	$0.304118*10^{-3}$
	Marcuse	$0.734241*10^{-5}$	$0.294801*10^{-2}$

Table 3. Comparison of present method with marcuse's radiation loss method ($k_0=d_1=1.00$ and $k_0l=0.05$).

Power in the continuous spectrum		$d_2/d_1=1.05$	$d_2/d_1=2.00$
T	Present	$0.160898*10^{-1}$	0.559534
	Marcuse	$0.176586*10^{-1}$	0.584920
R	Present	$0.446487*10^{-5}$	$0.136037*10^{-2}$
	Marcuse	$0.553715*10^{-5}$	$0.299040*10^{-2}$

agreement for the small step junction ($d_2/d_1=1.05$), but vary around 4% for large step junction ($d_2/d_1=2.00$). For the large step junction ($d_2/d_1=2.00$), the error in total power calculated from two methods of Marcuse based on the two different assumptions each is 0.8%, which is almost coincident with those from the present method.

Marcuse's methods is effective for small step junction but moderate for a large step junction. Moreover, there is no way of improving the accuracy in his method. In the present method, the accuracy of numerical results could be improved by increasing the number of expansion terms taking for the computation.

〈5·2〉 Multi-stages (tapered dielectric waveguide) As an example, we describe the numerical charcteristic of the cascading stages to 4, where each stage consists of the single step junction of two different dielectric waveguide followed by the short waveguide section. The dimension of each transmission matrix is selected so as to be the same. According to Eq. (37), $[{}_{\mathrm{I}}\Omega_{\mathrm{II}}]$, $[{}_{\mathrm{I}}\Omega_{\mathrm{II}}][{}_{\mathrm{II}}\Omega_{\mathrm{III}}]$, $[{}_{\mathrm{I}}\Omega_{\mathrm{II}}][{}_{\mathrm{II}}\Omega_{\mathrm{III}}][{}_{\mathrm{III}}\Omega_{\mathrm{IV}}]$, and $[{}_{\mathrm{I}}\Omega_{\mathrm{II}}][{}_{\mathrm{II}}\Omega_{\mathrm{III}}][{}_{\mathrm{III}}\Omega_{\mathrm{IV}}][{}_{\mathrm{IV}}\Omega_{\mathrm{V}}]$ are numerically calculated. Using these transmission matrices, we can obtain the expansion coefficients of mode amplitude each. The normalized power transferred into the continuous mode is calculated when the dominant mode HE_{11} is applied in the waveguide at $k_0d=1.00$.

Fig. 5 shows the comparison of the results by the present method with those by Marcuse's approximate radiation loss method. According to Fig. 5, radiation

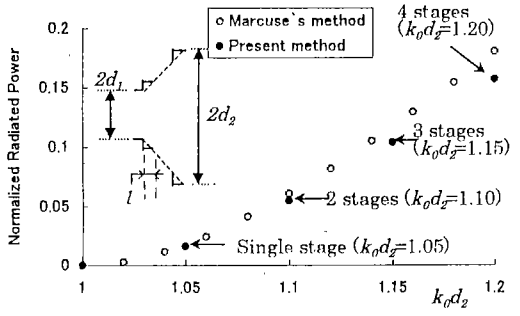

Fig. 5 Normalized radiated power vs number of stages (k_0d_1=1.00, k_0l=0.05, cone-flare angle 45°).

from the cascaded stage is reasonably increasing with the number of stages when cone-flare angle is constant. Fig. 5 also shows that the present method and Marcuse's one predict almost same radiation loss in the case of the single stage and two stages. However, when the number of stages is increasing, the discrepancy of the results from both methods is greater. It is considered that this is due to the cause of several assumptions in Marcuse's method in order to treat the problem easily.

6. Conclusions

A rigorous multiport representation for a symmetric step junction of two circular dielectric waveguides was given and tested numerically for the power conservation. Present results were compared with those obtained from approximate methods given by Marcuse. Both results showed agreement in the case of a small step size but showed considerable variation for the large steps. It is due to facts that Marcuse has neglected the reflected components of the continuous mode while formulating the mode-matching method, and in his radiation-loss method, he has made further assumptions in addition to neglecting the reflected component of discrete modes. The present method is included many time-consuming calculation processes compare to Marcuse's method but it is a comprehensive and rigorous method, because in the present method the required accuracy for computation could be achieved by increasing the number of expansion terms taking for the computation for any kind of symmetric step junctions.

A tapered dielectric waveguide was analyzed by stepwise approximation using the multiport representation of the symmetric step-junction of circular dielectric waveguides. The comparison of the present method and Marcuse's radiation-loss method was also given. The present stepwise approximation method is applicable to any symmetric tapered dielectric waveguide and gives fundamentals of the design of such a waveguide.

(Manuscript received Jan. 29, 2001, revised July 30, 2001)

References

(1) C. Salema, C. Fernandes & R. K. Jha: Solid dielectric horn, Ch. 6 (1998) Artech House

(2) A. W. Snyder, "Surface Mode Coupling along a Tapered Dielectric Rod," *IEEE Trans. AP*, **13**, 821～822 (1965)

(3) A. W. Snyder: "Coupling of Modes on a Tapered Dielectric Cylinder," *IEEE Trans. MTT*, **18**, 383～392 (1970)

(4) D. Marcuse: "Radiation Losses of the Dominant Mode in Round Dielectric Waveguide," *Bell System Technical J.* **49**, 1665～1693 (1970)

(5) S. F. Mahmoud & J. C. Beal: "Scattering of Surface Waves at a Dielectric Discontinuity on a Planar Waveguide," *IEEE Trans. MTT*, **23**, 193～198 (1975)

(6) M. Guglielmi, G. Gheri, M. Calamia & G. Pelosi: "Rigorous Multimode Network Numerical Representation of Inductive Step," *IEEE Trans. MTT*, **42**, 317～326 (1994)

(7) T. E. Rozzi: "Rigorous Analysis of the Step Discontinuity in a Planar Dielectric Waveguide," *IEEE Trans. MTT*, **26**, 738～746 (1978)

(8) N. S. Kapany & J. J. Burke: Optical Waveguide, Ch. 4 (1972) Academic Press

(9) N. Morita: "Radiation Modes of Circular Dielectric Waveguides," *J. Electromagnetic Waves & Applications*, **2**, 445～457 (1988)

(10) G. Goubau & F. Schwering: "On the Guided Propagation of Electromagnetic Wave Beams," *IEEE Trans. AP*, **AP-9**, 248～256 (1972)

(11) K. Pirapaharan & N. Okamoto,: "A Multiport Representation of the Step Junction of Two Circular Dielectric Waveguides," *IEICE Trans. Electronics*, **E84-C**, no. 11, 1697～1702 (2001)

Pirapaharan Kandasamy (Non-member)

He received the B. Sc. Eng. degree (with honors) in electrical and electronic engineering from the University of Peradeniya, Sri Lanka, in 1993, the M. Eng. and D. Eng. degrees in electronic engineering from Kinki University, Japan, in 1998 and 2001, respectively. He is currently a Postdoctoral Research Associate with University of Illinois at Urbana-Champaign, USA. His research interests include the area of computational electromagnetics.

Nobuo Okamoto (Non-member)

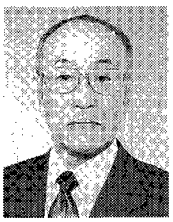

He was born in Osaka, Japan on September 22, 1934. He received the B. Eng., M. Eng., and D. Eng. degrees in electrical communication engineering from Osaka university, Osaka, Japan, in 1957, 1959, and 1967, respectively. In 1959, he joined the Department of Science and Technology, Kinki University, where, since 1970, he has been a Professor. His research has included electromagnetic fields in systems containing gyrotropic materials and electromagnetic circuits in the millimeter-and sub-millimeter-wave regions. He co-authored Electromagnetics (Tokyo, Japan: Corona, 1979) and Electromagnetic Waves and Communication Engineering (Tokyo, Japan: Kyouritsu Shuppan, 1988). Dr. Okamoto is the member of the Institute of Electronics, Information and Communication Engineers, Japan, and the Japan Society of Applied Physics. He is also a life member of The Institute of Electrical and Electronic Engineers (IEEE).